Published in final edited form as:
Nat Struct Mol Biol. 2010 May ; 17(5): 596–601. doi:10.1038/nsmb.1795.

Structures of apicomplexan calcium-dependent protein kinases reveal mechanism of activation by calcium

Amy K. Wernimont[1], **Jennifer D. Artz**[1], **Patrick Finerty Jr.**[1], **Y. Lin**[1], **Mehrnaz Amani**[1], **Abdellah Allali-Hassani**[1], **Guillermo Senisterra**[1], **Masoud Vedadi**[1], **Wolfram Tempel**[1], **Farrell Mackenzie**[1], **Irene Chau**[1], **Sebastian Lourido**[2], **L. David Sibley**[2], and **Raymond Hui**[1,3]

[1]Structural Genomics Consortium, University of Toronto, MaRS South Tower, Suite 732, 101 College St., Toronto, Ontario, Canada M5G 1L7

[2]Department of Molecular Microbiology, Washington University School of Medicine, 660 S. Euclid Avenue, St Louis, Missouri 63110, USA. 2Donald Danforth Plant Science Center, 975 N. Warson Road, St Louis, Missouri 63132, USA

Abstract

Calcium-dependent protein kinases (CDPKs) play pivotal roles in the calcium-signaling pathway in plants, ciliates and apicomplexan parasites, and comprise a CaMK-like kinase domain regulated by a calcium-binding domain in the C-terminus. To understand this intramolecular mechanism of activation, we solved the structures of the autoinhibited (*apo*) and activated (calcium-bound) conformations of CDPKs from the apicomplexan parasites *Toxoplasma gondii* and *Cryptosporidium parvum*. In the *apo* form, the C-terminal CDPK activation domain (CAD) resembles a calmodulin protein with an unexpected long helix in the N-terminus that inhibits the kinase domain in the same manner as CaMKII. Calcium binding triggers the reorganization of the CAD into a highly intricate fold, leading to its relocation around the base of the kinase domain to a site remote from the substrate-binding site. This large conformational change constitutes a distinct mechanism in calcium signal transduction pathways.

Apicomplexan parasites are a diverse group of protozoan parasites, several of which cause important human and animal diseases. They are united by a conserved set of specialized apical organelles – e.g. the rhoptry and micronemes – and a shared mechanism of actin-based motility that is essential for active penetration of their host cells[1]. Calcium controls a number of essential pathways in these parasites including protein secretion, activation of motility, cell invasion and egress[2]. Similar to other eukaryotes, apicomplexan organisms employ EF-hand containing proteins as calcium sensors, including a group of calcium-dependent protein kinases (CDPK) also found in plants and ciliates but not in animals or fungi. The canonical CDPK comprises a calcium-binding domain of 4 EF-hands attached to the C-terminus of a kinase domain that is highly homologous to calmodulin-dependent kinases (CaMK). Whereas CaMKs are autoinhibited by a C-terminal helix[3], CDPKs are

[3]Correspondence and requests for materials should be addressed to R.H. (raymond.hui@utoronto.ca).

Author Contributions Y.L. and M.A. purified, crystallized the proteins and performed mass spec analyses. A.K.W. and W.T. collected and processes x-ray data. A.K.W., J.D.A. and R.H. designed the experiments and analyzed the results. A.K.W. refined and analyzed the structural models. F.M. cloned the constructs. S.L. and L.D.S. identified the entry clone for TgCDPK1. L.D.S. provided functional analysis. P.F., A.A., G.S. and I.C. conducted various assays on the proteins and analyzed the results. M.V. was also involved in analysis of assay results.

The authors declare no competing financial interests.

Accession codes. Protein Data Bank: Coordinates for a-TgCDPK1, i-TgCDPK1, i-TgCDPK1 and a-CpCDPK1 have been deposited with the accession codes 3HX4, 3KU2, 3HZT and 3IGO respectively.

regulated by their calcium-binding domain. Specifically, in response to transient increases in the level of cellular calcium, CDPKs undergo conformational changes that activate their ability to regulate the other proteins by means of phosphorylation. So far, these serine/threonine kinases have been implicated in specific functions and development of distinct stages in the complex life cycles of apicomplexan parasites, based on chemical and genetic experiments[4]; however, the precise roles played by individual CDPKs remain largely undefined in both plants and parasites.

CaMKs and CDPKs are not the only kinases with integral regulatory domains. Protein kinase C (PKC) features an amino-terminal regulatory domain that includes an inhibitory pseudosubstrate motif and activates the kinase domain upon binding diacylglycerol and calcium. Rhoptry kinases in *Toxoplasma gondii* have an N-terminal arm blocking the ATP-binding site until it is autophosphorylated at specific positions[5]. Abl and Src tyrosine kinases are regulated by interaction between the kinase domain and the N-terminal SH2 and SH3 domains[6,7]. Despite the availability of information on these and other kinases, various studies on CDPKs[8,9] suggest they are regulated by a distinctive mechanism, which remains a subject of speculation.

To shed light on this mechanism of activation, we present the structures of three CDPKs from the apicomplexan parasites *Toxoplasma gondii* and *Cryptosporidium parvum*, namely TgCDPK1, CpCDPK1 and TgCDPK3 (naming scheme follows Billker et al[4]). The first two proteins are respectively the *Toxoplasma* and *Cryptosporidium* orthologues of *Plasmodium* CDPK4[4,9,10], previously implicated in malarial gamete formation[10]. The third protein in our study, namely TgCDPK3, is an orthologue of PfCDPK1, which has been found to phosphorylate substrates involved in host invasion[11]. All three proteins feature the canonical arrangement of a kinase domain followed by 4 EF-hands (sequence alignment and key motifs shown in Supplementary Figure 1), making them representative models for the majority of CDPKs in plants and parasites.

Results

Characterization of the Effect of Calcium on CDPKs

We tested the activity of TgCDPK1, CpCDPK1 and TgCDPK3 as a function of calcium using the PK-LDH assay[12] with Syntide 2 (a common CaMK substrate with the sequence PLARTLSVAGLPGKK) as a peptide substrate[9,13]. All exhibited a level of phosphorylation activity increasing with Ca^{2+} concentration, with activation constants determined to be 10, 14 and 14 μM respectively (Figure 1a).

To study whether calcium-induced activation is reversible and requires continuous presence of Ca^{2+}, we conducted a “calcium in-out-in” experiment. The proteins were incubated in $CaCl_2$, $MgCl_2$ and ATP for an hour to allow for activation and potential autophosphorylation. Subsequently, an aliquot of each was taken to confirm full activity. The remaining activated samples were treated with EDTA and extensively dialyzed to remove Ca^{2+}: this resulted in lower levels of activity, with the two *Toxoplasma* CDPKs partially active whereas the *Cryptosporidium* enzyme showed only a basal level of function. Subsequently, $CaCl_2$ was added again to the samples, with all three almost completely restored to their maximum level of activity (Figure 1b). These results suggest that, under the conditions tested, some but not all CDPKs can be fully inactivated by removing calcium alone.

Structural Biology

To study the inactivated state of CDPKs, we obtained crystal structures of TgCDPK1 and TgCDPK3, respectively at 2.3 and 2.0Å (Table 1), with the kinase domain (KD) and EF-

hands intact but without adding calcium. Both structures, henceforth referred to as i-TgCDPK1 and i-TgCDPK3 to denote their inactivated enzymatic state (Figures 2a and 2b), feature a canonical bilobed kinase domain (KD) and a regulatory domain dubbed the CDPK activation domain (CAD). The CAD starts a few residues downstream of a highly conserved HXW motif (X being most often proline including in TgCDPK1 and TgCDPK3). The first part of the CAD emanates from the base of the KD in the form of a long helix (named CH1 herein and shown in cyan in Figure 2), extending between the C-termini of helices αD and αF (following common kinase nomenclature). Beyond CH1, the CAD spans the N-EF-lobe and a second long helix dubbed CH2, and ends after the C-EF-lobe. It shares above 30% sequence identity with CaM as well as human troponin C (TnC) and largely resembles the dumbbell shape of the closed form of these two EF-hand containing proteins but with an extra long helix added (Supplementary Figures 2 and 3). Past studies of the regulatory domain of CDPKs included only a C-terminal portion of CH1 and characterized the first half as an independent junction domain[9,14]; however, this mostly amphipathic helix is an integral component in its entirety and defines the overall CAD as a novel member of the EF-hand containing family. As described further below, additional structural evidence supports this distinction.

The CH1 helix can be divided into three segments. The first is the autoinhibitory region blocking substrate-binding site of the KD and extends a basic residue (Lys338 in i-TgCDPK1, which is used as the reference protein in the description of the inactivated CDPK unless otherwise specified) to interact with a conserved acidic cluster made up of E135 and D138 on helix αD (Figure 3a). The side-chain of E135 is turned towards the CH1 helix and prevents it from fulfilling its function of positioning the ATP ribose in the active site pocket. This Lys-Glu-Asp triad (with Arg being a frequent substitute for Lys) and the orientation of CH1 are conserved in parasitic and plant CDPKs, and are also characteristic of the pseudosubstrate inhibition mode observed in CaMKII[3]. The residues Lys338 and Leu339 mark the transition into the second segment, which also ends in a KL pair and contributes hydrophobic residues, namely Leu339, Met347 and Leu351, to the latter's hydrophobic core. All three residues are conserved in CDPKs, with Leu339 and Met347 also conserved in different isoforms of CaMKII and participating in key hydrophobic interaction with calmodulin[15]. Finally, the last segment of the CH1 helix serves as the E-helix of the first EF-hand, namely E1 (Supplementary Figure 1 and Figures 2a and 2b), with Leu360, Phe364 and Met367 engaged in the hydrophobic core of the N-EF-lobe.

From the N-EF-lobe onward, the inactivated form of the CAD largely resembles CaM in structure and organization (Supplementary Figures 2 and 3). The CH2 helix emerges from the second EF-hand to run almost anti-parallel to CH1 but is comparatively shorter by the length of the autoinhibitory segment. It can also be divided into three segments: the F-helix of the second EF-hand (F2) and the E-helix of third EF-hand (E3) form the bookends, with a linker in the middle that is similar to but shorter than that found in CaM and TnC. Interestingly, in i-TgCDPK1 and i-TgCDPK3, both CH1 and CH2 are slightly bent, with the two helices bowed towards each other in a manner presaging this region's potential conformational change.

In addition to the Lys-Glu-Asp triad, there are at least three other regions implicated in binding the KD and CAD in the inactivated state. First, Leu323, Ile327, Ile330 and Phe333 (conserved as identical or similarly hydrophobic residues in other parasitic CDPKs) on CH1 are buried in the amphipathic cleft in the C-terminal lobe of the KD, anchoring the long helix in place (Figure 3d). In addition, the N-lobe of the KD interacts with an insert in the N-EF-lobe of the CAD (Figures 3a and 3b) – an insert found in a number of CDPKs but not CaM or TnC (see Supplementary Figure 1). Finally, both the activation segment of the KD (between the DFG and APE motifs) and the helix αC are in their respective inactive

positions, with the activation segment thus locked by an isoleucine (Ile212) extended into a hydrophobic pocket in the interface between CH1 and the C-EF-lobe (Figure 3b). Both the isoleucine and the residues forming the pocket are conserved amongst many apicomplexan and plant CDPKs Along with the hydrophobic cores in the two EF-lobes, these three regions stabilize the inactivated CDPK conformation.

We also obtained the calcium-bound structures of TgCDPK1 and CpCDPK1, respectively resolved at 1.9 and 2.1 Å, with the KD and CAD intact (Table 1). They represent the activated conformation of CDPKs and are therefore referred to as a-TgCDPK1 and a-CpCDPK1 below. In comparison to i-TgCDPK1 and i-TgCDPK3, it is easily noticeable that the entire CAD is translocated to a new position roughly 135° clockwise from its inactivated position about the KD (Figures 2e and 2f). Unforeseen in previous studies of CDPKs, this movement liberates the residues required for activity and substrate recognition. Furthermore, with the CAD out of the way, helix αD is now positioned much closer to helix αF, closing the cleft at the base of the KD where the CH1 is anchored in the autoinhibited structure (Figures 3e).

Calcium binding also induces the CAD to undergo substantial refolding. In both the a-TgCDPK1 and a-CpCDPK1 structures, all four EF-hands coordinate Ca^{2+} (Figures 2c and 2d), resulting in the opening of these subdomains, exposure of hydrophobic surfaces and subsequent refolding of the entire activation domain. The CH1 and CH2 helices are no longer anti-parallel. Instead, they are partially unwound and bent at the boundaries between the above defined segments, and intricately intertwined around each other and engaged in hydrophobic interaction with the two calcium-loaded EF-lobes (Figures 2c and 2d). Interestingly, the autoinhibitory region in the CH1 helix, previously found in hydrophobic interaction with the C-EF-lobe in the autoinhibited state, is now involved in similar interaction with the N-EF-lobe. This highlights the range of the CAD rearrangement, which is more extensive than that seen in calmodulin and made possible because the involvement of the entire CH1 helix makes available more surfaces for interaction in comparison to other EF-hand containing domains.

Driven out of its autoinhibitory position, the CAD finds itself lodged on a different face of the KD, secured by a different set of contacts (Figure 3c). The N-EF-lobe, which lines up next to the N-lobe of the KD in the inactivated state, is now next to the C-lobe instead, with salt bridges formed between the backbone nitrogens of ^{424}TS^{425} and the side-chain of Asp107, which is just downstream of helix αC. All three residues are highly conserved with the TS pair situated on the tail end of the second EF-hand (DFDKNGYIEYSE), wherein calcium coordination has imposed a particular geometry to expose the backbone nitrogens to the surface. In another contact between the domains, the E3 helix in the C-EF-lobe extends Arg445 (highly conserved as Arg, Lys or Gln in apicomplexan CDPKs but not in plant CDPKs) into a negatively charged pocket on the KD surface to form salt bridges with Asp70 and Glu116 (with the aspartate conserved amongst parasites and plants but the glutamate conserved only in parasites). Additional backbone interactions are found between ^{349}SY^{350} and ^{113}KL^{114}. This KL motif is conserved throughout parasitic CDPKs as well as some plant CDPKs (with lysine replaceable by arginine and leucine by isoleucine); however, the SK pair is only preserved for a small subset of parasitic CDPKs and not at all in plants. The ^{338}KL^{339} pair in the pseudosubstrate segment on CH1 is also engaged, with Leu339 again occupied in the hydrophobic core of the C-EF-lobe. Interestingly, Lys338 forms a hydrogen bond with the backbone oxygen of Leu32, which is part of a N-terminal stretch (30 residues from the beginning of the full length protein and shown in green in Figure 3c) latching first onto a hydrophobic ridge and then between the second EF-hand motif and the C-terminal EF-hands (Figure 3c). This N-terminal region is missing in the a-CpCDPK1

structure; however, sequence alignment suggests it is conserved in this kinase and some other apicomplexan CDPKs.

Discussion

The extent of the structural rearrangement in CDPKs resulting from binding calcium is, insofar as we know, unprecedented amongst kinases (Figure 4a), surpassing the movement of the SH2 and SH3 domains in tyrosine kinases. The CAD is also capable of more twists and turns than other proteins containing EF-hands such as CaM[16] (Figures 4b and 4c) in part because it is a larger domain with on average about 200 amino acids, compared to 148 for calmodulin (Supplementary Figure 2). The additional length is located primarily in the CH1 helix, as well as inserts specific to each protein. As in CaM and TnC, the activated CAD is held together by extensive hydrophobic interaction, featuring methionine and, more prominently in CDPKs, leucine. More importantly, unlike CaM and TnC, the purpose of the CAD rearrangement is not to engage a substrate protein. Instead, we propose that the bending of CH1 and CH2 helices and their entanglement with the EF-hands drive the whole domain away from the KD, severing the above-described KD-CAD interfaces, including and specifically the autoinhibitory triad of Lys-Glu-Asp. This process makes Glu135 available to interact with ATP, allows the activation loop to assume the active orientation, removes occlusion from the substrate binding state and frees the helix αC to approach the nucleotide-binding site. Other steps may still be required for complete activation; however, our enzymatic results as well as other published results indicate that calcium alone can activate many CDPKs.

CDPKs have other interesting sequence features in addition to the EF-hands. Specifically, the (K/R)L pair is a recurring motif amongst parasite and plant CDPKs, as well as within individual CDPKs (Supplementary Figure 1). In the N-lobe of the KD, ^{113}KL^{114} (numbering based on TgCDPK1) is engaged in interaction with the CAD in the activated structure. Interestingly, their interaction partner is the ^{349}SK^{350} pair, with Lys350 being part of ^{350}KL^{351}. The remaining pair, ^{338}KL^{339}, is also the most significant, with Lys338 as the key residue in the autoinhibitory mode and L339 participating in hydrophobic interaction with the C-EF-lobe. Ranjan et al[9] observed that in PfCDPK4, replacement of this leucine (Leu360 in PfCDPK4) with an alanine resulted in loss of activity, thus confirming the significance of this hydrophobic interaction and the CH1 helix as a whole.

Although CDPKs adopt the pseudosubstrate inhibition feature, they do not share all other important mechanistic features of CaMKs. First, there is no evidence in structure or sequence suggesting that CDPKs form an oligomeric complex similar to that adopted by CaMKII[3]. Second, unlike CaMKI and CaMKIV, phosphorylation by another kinase has so far not been found necessary for CDPK activation as seen in previous reports[9,17] and our own assays; however, the number of detailed biochemical studies on individual CDPKs still provide insufficient data for family-wide generalization. On the other hand, autophosphorylation is often necessary for activation of many kinases. In PfCDPK4, for example, autophosphrylation of Thr234 has been observed to be essential[9]. This threonine is part of a IGTAYY motif in the activation loop that is highly conserved in both parasitic and plant CDPKs. Therefore, autophosphorylation of the active loop may be a common requirement amongst CDPKs. Specific to CaMKIIs is autophosphorylation of Thr286 located at the base of the autoinhibitory helix, which takes place to maintain constitutive activity after initial activation. In another study[18], it was observed that this key threonine was not conserved amongst plant and *Plasmodium* CDPKs; however, we note that in most CDPKs, there are various serines and threonines situated in other positions between the HXW motif at the base of the C-lobe of the KD and the N-terminus of the CH1 helix. Covalent attachment of a phosphate group to anyone of these residues may potentially

prevent a CDPK's return to the inactivated state. Furthermore, autophosphorylation sites in the CAD have been identified in *Arabidopsis* and *Plasmodium* CDPKs[18], some of which may have the capacity to lock a kinase in the activated conformation even in the absence of calcium. Our "calcium in-out-in" experiments were designed to investigate this possibility, but produced mixed results – under the conditions tested, only CpCDPK1 can be toggled between the active and inactive states solely by manipulation of calcium levels. For TgCDPK1 and TgCDPK3, there are two possible interpretations: EDTA may be inadequate as a chelating agent or these two enzymes were modified by the process of calcium activation such that they were unable to fully return to their inactivated state. Additional research is required to determine whether some or most CDPKs share CaMK's ability to become constitutively active.

Based on sequence alignment, many of the structural features discussed herein, including pseudosubstrate inhibition and some of the KD-CAD interactions in both states, can be predicted to be conserved in other apicomplexan CDPKs as well as canonical CDPKs at large. What is unconserved is a small gatekeeper residue - glycine in TgCDPK1 and CpCDPK1, and serine in *Plasmodium* CDPK4. This is rare in native kinases and creates a hydrophobic pocket in the nucleotide-binding site (Supplementary Figures 1 and 4), which can be exploited for selective chemical inhibition [19,20].

Study of CaMKs has shown that their mechanistic behavior and function are highly related[21, 22]. It follows that structural and mechanistic discrepancies between CaMKs and CDPKs are also driven by functional divergence. Based on findings to date, CDPKs can be characterized as self-contained calcium sensors enaged in calcium pathways simpler than in animals in which extraneous proteins such as calmodulin and CaMKK are necessary to control the action of CaMKs. The selective use of CDPKs by ciliates and apicomplexans is particularly interesting, given that their genomes do not contain PKC and have relatively few CaMKs. These two groups are the dominant calcium-mediated kinases in other protists, most notably trypanosomatids[23] which do not share the apicomplexan method for host invasion. Future research will uncover specific mechanistic behavior of individual CDPKs and reveal how plants and parasites use the direct calcium-sensing properties of these kinases to their advantage.

Methods

Protein Expression

Information for all vectors used are available at http://www.sgc.utoronto.ca/SGC-WebPages/toronto-vectors.php. Using a full-length synthetic template purchased from Codon Devices (Cambridge, MA, USA) and reference sequence for the gene 541.m00134 in the ToxoDB database (www.toxodb.org), we subcloned a construct of TgCDPK3 truncated at the N-terminus (L72-H537) and appended with an *N*-terminal His_6tag including an integrated TEV cleavage site (mhhhhhhssgrenlyfq*g) into the pET15-MHL vector. A similarly tagged construct of CpCDPK1 (T71-E538) was subcloned from *Cryptosporidium parvum* strain Iowa genomic DNA (obtained from MR4, Manassas, VA, USA) also into the pET15-MHL vector. The full length TgCDPK1 cDNA was cloned into the same expression vector and also appended in the same way as the others. We expressed and purified all constructs as previously described[24] using the Lex bioreactor system (Harbinger Biotechnology and Engineering Corp., Markham, ON, Canada) and BL21(DE3)-V2R-pACYC LamP as the expression host, which includes a plasmid for co-expression of lambda phosphatase to suppress protein phosphorylation. EDTA was excluded from the purification protocol. All protein samples eluted as apparent monomers from a Superdex S200 gel filtration column (GE Life Sciences, Baie d'Urfe, QC, Canada). The identities of the purified constructs were

verified by mass spectroscopic analysis, which also confirmed the absence of phosphorylation.

Crystallography

TgCDPK3 crystals emerged in 20% PEG 3350 and 0.2M KF with the addition of 3mM 5-[(Z)-(5-chloro-2-oxo-1,2-dihydro-3H-indol-3-ylidene)-methyl]-N-[2-(diethylamino)ethyl]-2,4-dimethyl-1H-pyrrole-3-carboxamide (SU11652 from EMD Chemicals, Gibbstown, NJ, USA), and were flash frozen in N_2(l) with 25% glycerol as a cryoprotectant. For CpCDPK1, the conditions yielding the final crystals were 20% PEG 3350 and 0.2M diammonium tartrate in the presence of 2mM AMPPNP, 4mM $MgCl_2$, 2mM $CaCl_2$, and 6mM TCEP. These crystals were flash cooled in N_2(l) with 30% glycerol as a cryoprotectant. For the i-TgCDPK1 structure, crystals grew at 20 °C in 20% PEG 3350, 0.2M KF, 2mM AMPPNP, 4mM $MgCl_2$, 6.25mM TCEP. Crystals were flash cooled in N2(l) with 35% Peg 3350 as a cryoprotectant. For the activated form, TgCDPK1 was crystallized at 20 °C in 26% PEG 3350, 0.2M Li_2SO_4, and Tris buffer (pH 8.0) in the presence of 2mM AMPPNP, 4mM $MgCl_2$, 2mM $CaCl_2$, and 6mM TCEP. Crystals were flash cooled in N_2(l) with mother liquor supplemented with 30% glycerol.

We collected data for TgCDPK3 and a-TgCDPK1 at the APS beam line 19ID (http://www.sbc.anl.gov). Data for CpCDPK1 were collected on a rotating anode FR-E+ Superbright with a RAxis IV++ (Rigaku, The Woodlands, TX, USA). Data for i-TgCDPK1 were collected on a Rigaku rotating anode FR-E Superbright with a Rigaku Saturn A200 ccd detector. We processed all data using HKL-2000 (HKL Research Inc., Charlottesville, USA; www.hkl-xray.com) and solved all the structures first by molecular replacement using Phaser[25] and the TgCDPK3 kinase domain structure as the reference model (3DXN). The CAD domain was manually built in iterative stages using Coot and Refmac5 within the CCP4 program suite[26]. Final refinement for i-TgCDPK1 was done using the program *BUSTER-TNT* (Global Phasing Ltd., Cambridge, UK; www.globalphasing.com). Data processing and refinement statistics are summarized in Table 1. All structural representations in this paper were prepared with Pymol (Delano Scientific LLC, Palo Alto, USA; http://www.pymol.org) and espript (http://espript.ibcp.fr)

Calcium dependence assays

Kinase activity was measured using an NADH-coupled ATPase assay (using pyruvate kinase (PK) and lactate dehydrogenase (LDH)) in a 96-well format based on the method of Kilanitsa and adapted for use with high ATP concentrations[27]. After incubating ATP (1 mM) with the assay components (typically including 1 mM Syntide-2, 600 mM NADH, 200 mM PEP, LDH/PK mix from Sigma (with 6 units of LDH/mL), 10 mM $MgCl_2$, and $CaCl_2$, as indicated) for 10 minutes, the reaction was initiated with the addition of 125 nM enzyme. Initial rates were calculated (for 3 to 10 minutes) and triplicate data were analyzed using SigmaPlot 9.

For the “calcium-in-out-in” assay, each CDPK (1 μM) was incubated with 5mM $CaCl_2$, 5mM $MgCl_2$ and 1mM ATP in 25mM Tris, 200mM NaCl at pH 7.5. The mixture was incubated for 1 hour at room temperature. After incubation, 20mM EDTA was added, and the mixture was dialyzed overnight in 4 L of 25mM Tris, 200mM NaCl, pH 7.5 at 4°C. After testing for activity, 100 μM $CaCl_2$ was added and all the samples were tested for activity again. In summary, the different samples were assayed after initial incubation, after EDTA treatment and again after the second addition of calcium, all using the PK-LDH coupled assay with 1mM ATP and 1 mM Syntide-2.

Supplementary Material

Refer to Web version on PubMed Central for supplementary material.

Acknowledgments

We thank John Christodoulou at University College London, Oliver Billker at the Sanger Institute, Stefan Knapp, Tom Heightman, Matthieu Schapira, Cheryl Arrowsmith and Aled Edwards at the Structural Genomics Consortium (SGC) for insightful discussions and/or constructive review of this manuscript. We also thank Jocelyne Lew, Ashley Hutchinson, Abbasali Hassanali and Helen Ren at the SGC for their efforts in cloning and expressing the proteins in this study. The Structural Genomics Consortium (SGC) is a registered charity (number 1097737) that receives funds from the Canadian Institutes for Health Research, the Canadian Foundation for Innovation, Genome Canada through the Ontario Genomics Institute, GlaxoSmithKline, the Knut and Alice Wallenberg Foundation, the Ontario Innovation Trust, the Ontario Ministry for Research and Innovation, Merck & Co. Inc., the Novartis Research Foundation, the Petrus and Augusta Hedlund's Foundation, the Swedish Agency for Innovation Systems, the Swedish Foundation for Strategic Research, and the Wellcome Trust.

References

1. Sibley LD. Invasion strategies of intracellular parasites. Science. 2004; 304:248. [PubMed: 15073368]
2. Sibley LD. Intracellular parasite invasion strategies. Science. 2004; 304(5668):248. [PubMed: 15073368] Nagamune K, Moreno SN, Chini EN, Sibley LD. Calcium regulation and signaling in apicomplexan parasites. Subcell Biochem. 2008; 47:70. [PubMed: 18512342]
3. Rosenberg OS, et al. Structure of the autoinhibited kinase domain of CaMKII and SAXS analysis of the holoenzyme. Cell. 2005; 123(5):849. [PubMed: 16325579]
4. Billker O, Lourido S, Sibley LD. Calcium-dependent signaling and kinases in apicomplexan parasites. Cell Host Microbe. 2009; 5(6):612. [PubMed: 19527888]
5. Qiu W, et al. Novel structural and regulatory features of rhoptry secretory kinases in Toxoplasma gondii. EMBO J. 2009; 28(7):969. [PubMed: 19197235]
6. Cowan-Jacob SW, et al. The crystal structure of a c-Src complex in an active conformation suggests possible steps in c-Src activation. Structure. 2005; 13(6):861. [PubMed: 15939018]
7. Nagar B, et al. Structural basis for the autoinhibition of c-Abl tyrosine kinase. Cell. 2003; 112(6): 859. [PubMed: 12654251]
8. Chandran V, et al. Structure of the regulatory apparatus of a calcium-dependent protein kinase (CDPK): a novel mode of calmodulin-target recognition. J Mol Biol. 2006; 357(2):400. [PubMed: 16430916] Christodoulou J, Malmendal A, Harper JF, Chazin WJ. Evidence for differing roles for each lobe of the calmodulin-like domain in a calcium-dependent protein kinase. J Biol Chem. 2004; 279(28):29092. [PubMed: 15126505] Harmon AC, Putnam-Evans C, Cormier MJ. A Calcium-Dependent but Calmodulin-Independent Protein Kinase from Soybean. Plant Physiol. 1987; 83(4): 830. [PubMed: 16665348]
9. Ranjan R, Ahmed A, Gourinath S, Sharma P. Dissection of mechanisms involved in the regulation of plasmodium falciparum calcium dependent protein kinase 4 (PfCDPK4). J Biol Chem. 2009
10. Billker O, et al. Calcium and a calcium-dependent protein kinase regulate gamete formation and mosquito transmission in a malaria parasite. Cell. 2004; 117(4):503. [PubMed: 15137943]
11. Green JL, et al. The motor complex of Plasmodium falciparum: phosphorylation by a calcium-dependent protein kinase. J Biol Chem. 2008; 283(45):30980. [PubMed: 18768477]
12. Dolle C, Ziegler M. Application of a coupled enzyme assay to characterize nicotinamide riboside kinases. Anal Biochem. 2009; 385(2):377. [PubMed: 19027704]
13. Harmon AC, Yoo BC, McCaffery C. Pseudosubstrate inhibition of CDPK, a protein kinase with a calmodulin-like domain. Biochemistry. 1994; 33(23):7278. [PubMed: 8003491]
14. Yoo BC, Harmon AC. Intramolecular binding contributes to the activation of CDPK, a protein kinase with a calmodulin-like domain. Biochemistry. 1996; 35(37):12029. [PubMed: 8810907]
15. Meador WE, Means AR, Quiocho FA. Modulation of calmodulin plasticity in molecular recognition on the basis of x-ray structures. Science. 1993; 262(5140):1718. [PubMed: 8259515]

16. Chattopadhyaya R, Meador WE, Means AR, Quiocho FA. Calmodulin structure refined at 1.7 A resolution. J Mol Biol. 1992; 228(4):1177. [PubMed: 1474585]
17. Vitart V, et al. Intramolecular activation of a Ca(2+)-dependent protein kinase is disrupted by insertions in the tether that connects the calmodulin-like domain to the kinase. Biochemistry. 2000; 39(14):4004. [PubMed: 10747788]
18. Hegeman AD, et al. A phyloproteomic characterization of in vitro autophosphorylation in calcium-dependent protein kinases. Proteomics. 2006; 6(12):3649. [PubMed: 16758442]
19. Knight ZA, Shokat KM. Features of selective kinase inhibitors. Chem Biol. 2005; 12(6):621. [PubMed: 15975507]
20. Ojo KK, et al. A unique variation of the ATP binding site makes Toxoplasma gondii calcium-dependent protein kinase 1 a drug target for selective kinase inhibitors. Nature Structural and Molecular Biology. 2010
21. Braun AP, Schulman H. The multifunctional calcium/calmodulin-dependent protein kinase: from form to function. Annu Rev Physiol. 1995; 57:417. [PubMed: 7778873]
22. Hanson PI, Meyer T, Stryer L, Schulman H. Dual role of calmodulin in autophosphorylation of multifunctional CaM kinase may underlie decoding of calcium signals. Neuron. 1994; 12(5):943. [PubMed: 8185953]
23. Parsons M, Worthey EA, Ward PN, Mottram JC. Comparative analysis of the kinomes of three pathogenic trypanosomatids: Leishmania major, Trypanosoma brucei and Trypanosoma cruzi. BMC Genomics. 2005; 6:127. [PubMed: 16164760]
24. Vedadi M, et al. Genome-scale protein expression and structural biology of Plasmodium falciparum and related Apicomplexan organisms. Mol Biochem Parasitol. 2007; 151(1):100. [PubMed: 17125854]
25. Terwilliger T. SOLVE and RESOLVE: automated structure solution, density modification and model building. J Synchrotron Radiat. 2004; 11(Pt 1):49. [PubMed: 14646132]
26. Emsley P, Cowtan K. Coot: model-building tools for molecular graphics. Acta Crystallogr D Biol Crystallogr. 2004; 60(Pt 12 Pt 1):2126. [PubMed: 15572765]
27. Kiianitsa K, Solinger JA, Heyer WD. NADH-coupled microplate photometric assay for kinetic studies of ATP-hydrolyzing enzymes with low and high specific activities. Anal Biochem. 2003; 321(2):266. [PubMed: 14511695]

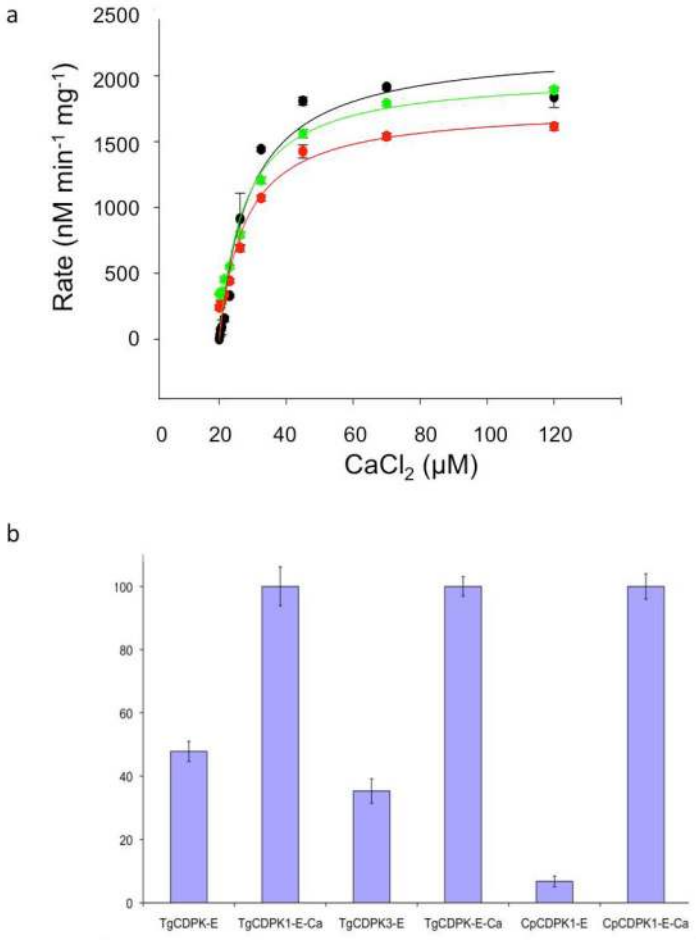

Figure 1. Effect of Ca^{2+} on CDPKs

(a) Using the LDH/PK assay and Syntide 2 as a substrate, all three enzymes were tested for activity in the presence of $MgCl_2$ and ATP with increasing Ca^{2+} concentration. For TgCDPK1 (black), K_m was found to be 10.2±1.6 μM. For TgCDPK3 (green), K_m found to be 14.0±2.0 μM. For CpCDPK1 (red), K_m was found to be 14.1±0.4 μM. (b) Calcium dependence experiment: Each CDPK (1 μM) was incubated with $CaCl_2$, $MgCl_2$ and ATP for 1 hour for activation and autophosphorylation. Afterwards, each sample was treated with EDTA and thoroughly dialyzed to remove Ca^{2+}. Two samples (labeled TgCDPK1-E, TgCDPK3-E, in the bargraph) demonstrated partial activity while CpCDPK1-E demonstrated only a basal level of activity. Calcium was added to all three samples again for activation, with all found to be fully active (TgCDPK1-E-Ca, TgCDPK3-E-Ca and CpCDPK1-E-Ca in the bargraph).

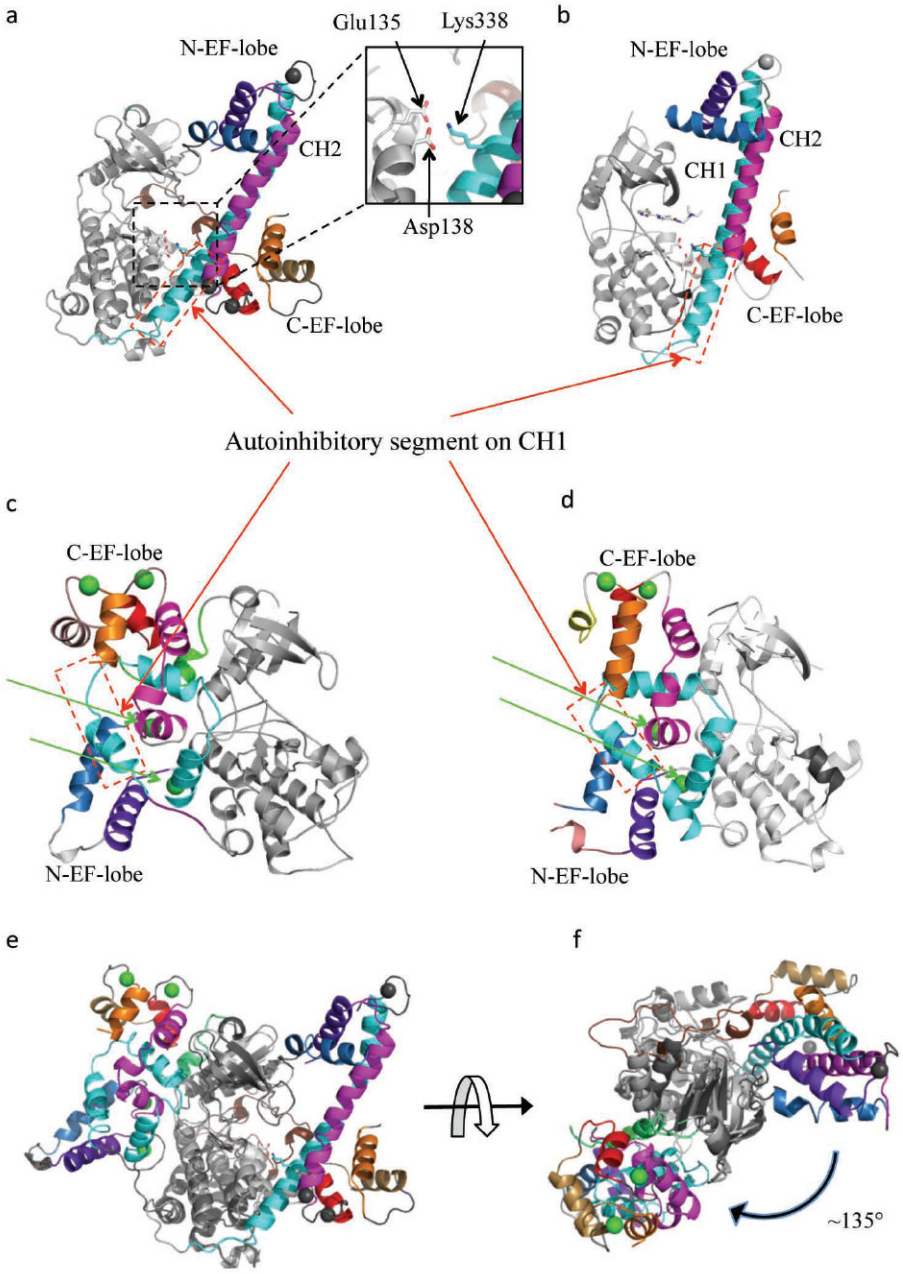

Figure 2. Crystal structures of apicomplexan CDPKs

The first four structures (a, b, c and d) are oriented by aligning their kinase domains. The kinase domain (KD) is shown in grey in all cases, with the CDPK activation domain (CAD) shown in color. The CH1 and CH2 helices are highlighted in cyan and pale magenta respectively, with these helices broken into three segments in the activated conformation (a-CpCDPK1 and a-TgCDPK1). The N-terminal latch in TgCDPK1 is shown in green. Calcium ions are shown as green spheres, with those hidden in the protein structures indicated by green arrows. (a) i-TgCDPK1 – structure of TgCDPK1 in inactivated conformation. A metal ion was observed in three of the four EF hands. The coordination of each did not match that of Ca^{2+} or Mg^{2+}. The pseudosubstrate autoinhibitory triad is highlighted. (b) i-TgCDPK3 – structure of TgCDPK3 in inactivated conformation. A Mg^{2+}

ion was found in one of the EF-hands in the C-terminus. (c) a-TgCDPK1 – structure of TgCDPK1 in activated conformation with 4 Ca^{2+} bound (green spheres). (d) a-CpCDPK1 – CpCDPK1 structure in activated conformation with 4 Ca^{2+} bound. (e) Cartoon schematic of i-TgCDPK1 and a-TgCDPK1 superimposed with the KD aligned, showing that the CAD has translocated from one side to the other. (f) Cartoon schematic of i-TgCDPK1 and a-TgCDPK1 superimposed with the KD aligned, as seen looking “down” at the beta lobe and showing the extent the translocation of the CAD around the KD.

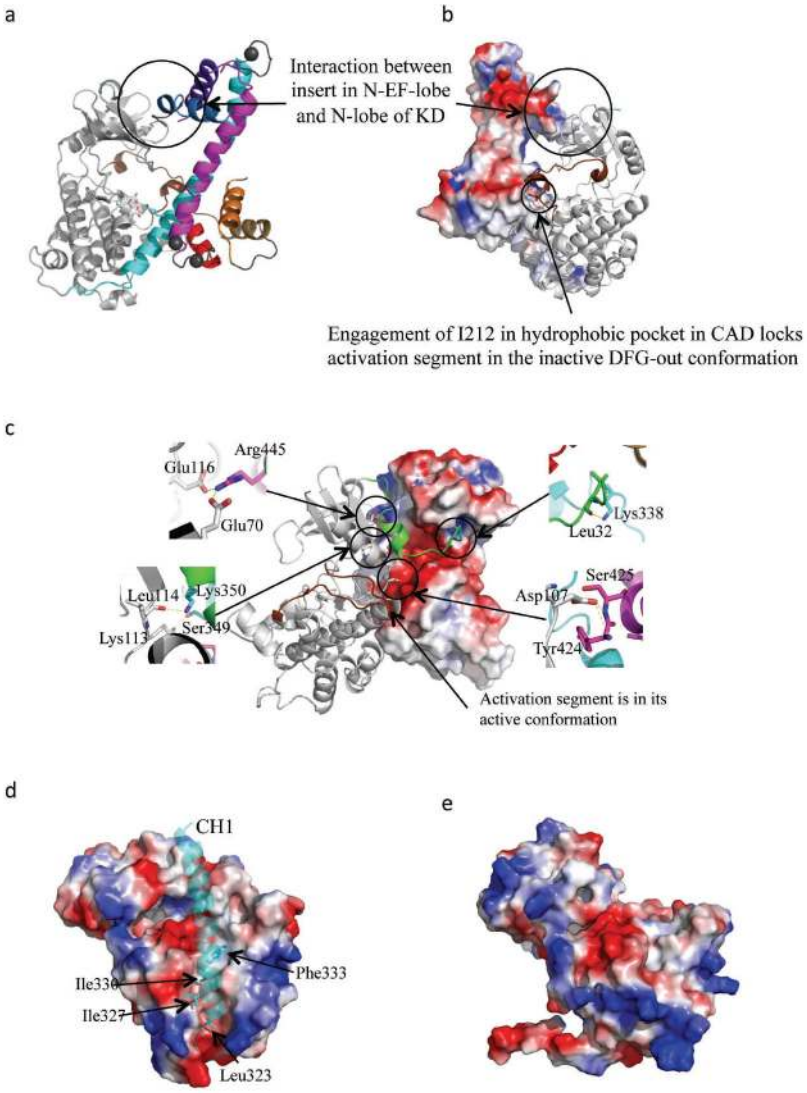

Figure 3. KD-CAD interfaces

(a) The insert in the N-EF-lobe is highlighted by a black circle, showing that it is in close proximity to the KD in the i-TgCDPK1 structure. (b) The interface between the insert in the N-EF-lobe and the KD is seen from "the other side" of the i-TgCDPK1 structure. Also shown is the brown activation segment locked in its inactive conformation by the engagement of I212 in a hydrophobic pocket in the surface of the CAD. (c) The key interfaces between the KD and the CAD in the activated conformation of TgCDPK1 are shown. The green helix in the N-terminus is latched into the CAD. The activation segment is free to move into its active conformation. (d) In the inactivated conformation, the CH1 helix (cyan) in the CAD has a number of hydrophobic residues buried in the amphipathic cleft at the base of the C-lobe of the KD. (e) In the activated conformation, the cleft has closed because the CAD, including the CH1 helix, has translocated to a different side of the KD.

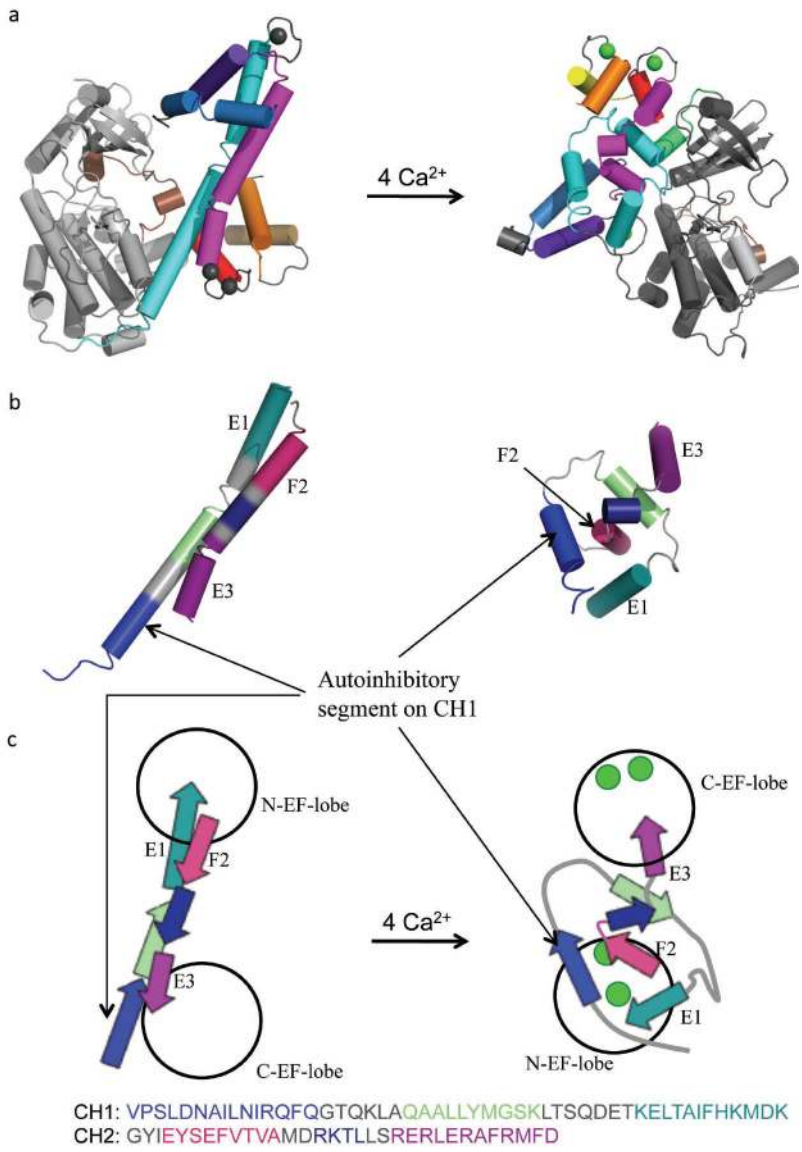

Figure 4. Schematic representing the activation of a canonical CDPK

(a) Cartoon schematic showing the inactivated (left) and activated (right) structures of TgCDPK1, with helices rendered as cylinders – The color scheme follows that used in Figures 2 and 3. (b) Cartoon schematic showing only the CH1 and CH2 helices in the calcium-absent (left) and calcium-loaded forms of the CAD – A new color scheme is used here to facilitate matching of the corresponding segments in the two states. The grey segments are those that unwind and bend in the transition from the inhibited state to the activated state. The amino acid sequences of the two helices are also shown in the same color scheme. (c) Simplified schematic of the CAD in the inactivated (left) and activated (right) states – The color scheme follows that used in Figure 4b. The green circles represent the calcium ions. The large circles represent the EF-lobes.

Table 1

Crystallographic table for all four protein structures

	i-TgCDPK1	a-TgCDPK1	i-TgCDPK3	a-CpCDPK1
Data collection				
Space group	P21	P212121	P21	P21
Cell dimensions				
a, *b*, *c* (Å)	48.01, 72.91, 65.02	49.24, 95.61, 101.61	71.05, 43.76, 84.82	60.48, 55.51, 81.71
α, *β*, *γ* (°)	90.00, 96.26, 90.00	90.00, 90.00, 90.00	90.00, 96.95, 90.00	90.00, 105.44, 90.00
Resolution (Å)	20-2.3 (2.34-2.30)	50-1.9 (1.97-1.90)	30-2.0(2.03-2.00)	50-2.25(2.33-2.25)
R_{sym} or R_{merge}	5.9 (39.5)	6.4 (84.2)	4.8 (45.7)	8.9 (87.8)
$I / \sigma I$	18.1 (1.2)	34.4 (1.2)	26.6 (2.7)	16.6 (1.7)
Completeness (%)	99.5 (94.4)	99.8 (98.1)	99.7 (99.6)	100 (99.9)
Redundancy	3.5 (2.4)	6.1 (3.7)	3.6 (3.3)	3.6 (3.5)
Refinement				
Resolution (Å)	20.0 - 2.3	50.0 – 1.95	50.0 – 2.0	50.0 – 2.25
No. reflections	19811	35714	33611	23815
R_{work} / R_{free}	0.201/0.238	0.209/0.257	0.212/0.253	0.201/0.255
No. atoms				
Protein	3592	3768	3481	3645
Ligand/ion	106	60	78	86
Water	78	195	203	125
B-factors				
Protein	55.08	24.1	42.12	28.405
Ligand/ion	72.057	45.22	39.75	66.61
Water	48.16	27.52	45.93	32.98
R.m.s. deviations				
Bond lengths (Å)	0.01	0.01	0.01	0.019
Bond angles (°)	1.1	1.2	1.2	1.9

N.B. For each structure, a single crystal was used.